Annu. Rev. Astron. Astrophys. 1993. 31: 63–92

PROTO-PLANETARY NEBULAE

Sun Kwok

Department of Physics and Astronomy, University of Calgary, Calgary, Alberta, Canada T2N 1N4

KEY WORDS: planetary nebulae, asymptotic giant branch, mass loss, circumstellar shells, radiative transfer, stellar evolution

INTRODUCTION

The evolutionary stage between the end of the asymptotic giant branch (AGB) and planetary nebula (PN) phases has long been a missing link in our understanding of single star evolution. As a star evolves up the AGB, it loses mass at an increasing rate until it is totally obscured by its own circumstellar dust envelope. At that time, the photosphere is no longer visible and the star appears as an infrared object. When mass loss reduces the mass of the hydrogen envelope (M_e) below a certain value ($M_e \sim 10^{-3}$ $M_\odot$ for a core mass M_c of 0.60 $M_\odot$, Schönberner 1983), the star will begin to evolve toward the blue side of the Hertzsprung-Russell (H-R) diagram. Soon after, the envelope is so depleted that large-scale mass loss is no longer possible. The effective temperature of the star will increase due to the loss of envelope mass as the result of hydrogen shell burning. This phase will last until the central star is hot enough ($T_* \sim 30{,}000$ K) to ionize the circumstellar nebula. Recombination lines of hydrogen and forbidden lines of metals will make the nebula easily observable in the visible. A new high-speed wind from the central star then compresses and shapes the AGB wind into a PN. A sketch of the evolutionary tracks of proto-planetary nebulae (PPN) in the H-R diagram is shown in Figure 1.

The difficulty in identifying PPN in the past was due to the fact that they are far infrared sources and very little is known about the far infrared sky; and if the PPN are visible, it has been difficult to distinguish them from ordinary stars. The situation changed as a result of the *IRAS* sky survey in 1983. Many far infrared sources were detected in the Galaxy and the hunt for PPN began almost immediately. In this review, I attempt to

0066-4146/93/0915-0063$02.00

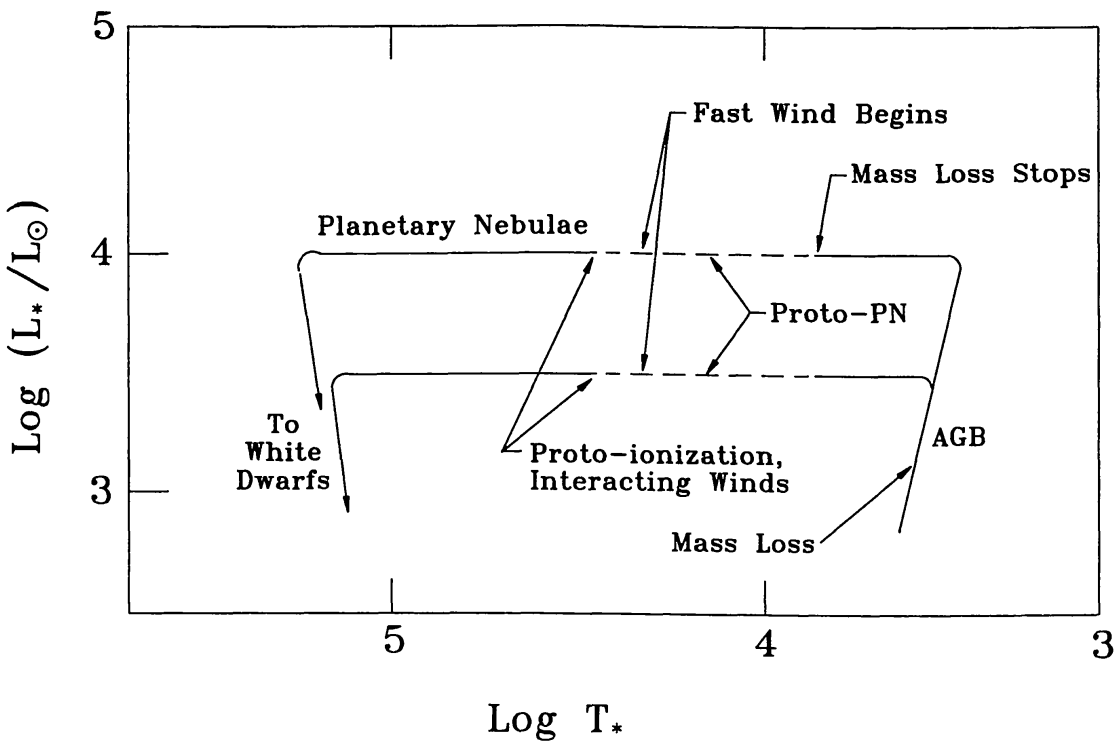

Figure 1 The proto-planetary nebula phase in the H-R diagram. The two tracks correspond to central stars of two different core masses.

report on the current status of the search for PPN, and to summarize the observational properties of these objects.

Definition of PPN

Since the term proto-planetary nebulae has been loosely used in the literature to refer to a variety of objects, ranging from evolved late-type stars on the AGB (e.g. IRC+10216) to young PNs (e.g. M2–9), we find it necessary to give this term a precise definition to restrict its use to stars that are in transition from the AGB to the PN phase. Specifically, we define PPN as stars that have stopped the large-scale mass loss on the AGB, but have not evolved to be hot enough to emit a sufficient quantity of Lyman-continuum photons to ionize the surrounding remnants of the AGB envelope.

Observationally, PPN candidates are expected to have the following properties:

1. A PPN candidate should show clear evidence of the remnant of the AGB envelope. These include: (*a*) large infrared excess with color temperatures between 150–300 K and (*b*) molecular emission (CO or OH) showing expansion velocity of 5–30 km s^{-1} typical of AGB winds.

2. There should be evidence that the circumstellar envelope is detached from the photosphere and is not the result of an ongoing mass loss process.
3. If the central star is bright enough for its spectral type to be determined, it should be primarily of spectral type B–G with luminosity class I.
4. There should not be large-amplitude photometric variability as the result of pulsation of a massive ($>10^{-3}\ M_{\odot}$) hydrogen envelope above the core.

Early PPN Candidates

The first PPN candidates, AFGL 618 and AFGL 2688, were discovered as the result of ground-based follow-up observations of objects in the Air Force Sky Survey. AFGL 618 is an infrared source of color temperature $\sim$200 K located in between two optical lobes separated by $\sim 7''$ in the east-west direction (Westbrook et al 1975). Visible spectropolarimetry shows the two lobes to be reflection nebulae (Schmidt & Cohen 1981) illuminated by a central star of spectral type BO. Radio continuum observations reveal a small ionized region of $0.4'' \times 0.1''$ embedded in the infrared source (Kwok & Bignell 1984). The entire optical nebula is surrounded by a molecular envelope of $\sim 20''$ which is expanding at 20 km s^{-1}, similar to circumstellar envelopes of AGB stars (Lo & Bechis 1976, Bachiller et al 1988). From the radial velocity structure, Carsenty & Solf (1982) have determined that the bipolar axis is inclined to the plane of the sky at an angle $\sim 45°$. The amount of extinction (A_v) is estimated to be $\sim$70–110 mag (Lequeux & Jourdain de Muizon 1990, Latter et al 1992).

AFGL 2688 (Egg Nebula), which was discovered by Ney et al (1975), is excited by a central star of spectral type F2-5 I (Crampton et al 1975). Its optical bipolar lobes extend over $10''$. Millimeter wave interferometric observations show that the CO envelope is centered on the infrared source and extends over $30''$ (Heiligman 1986).

The most plausible explanation for the nature of AFGL 618 and AFGL 2688 is that they are post-AGB objects evolving toward the PN stage. The infrared and molecular emissions originate from the remnants of the envelopes of their AGB progenitors. The envelopes are not spherically symmetric and the central stars are heavily obscured by circumstellar dust in the equatorial plane. The smaller optical thickness at the poles allows the visible light to escape, and the scattered light forms a bipolar nebula. Although the distances to these objects are uncertain, the observed luminosities [1.2×10^4 and 1.4×10^3 (D/kpc)^2 $L_{\odot}$ for AFGL 618 and AFGL 2688 respectively (Hrivnak & Kwok 1991a)], are consistent with their being post-AGB objects. In AFGL 618, the central star is probably more massive (therefore evolved faster) and is now just hot enough to begin to ionize the circumstellar environment. A steady increase in the free-free continuum flux level of AFGL 618 in the 21 cm to 800 μm range suggests that the ionized region began to form about 20–50 years ago (Kwok & Feldman 1981, Knapp et al 1993). Fast winds have been initiated, as evidenced by the broad CO wings (AFGL 618: Gammie et al 1989, Cernoicharo et al 1989; AFGL 2688: Young et al 1992, Jaminet et al 1992), as the first step toward the formation of a PN (Kwok et al 1978).

PPN AS TRANSITION OBJECTS

Since the PPN phase represents a short ($\sim 10^3$ yr) evolutionary phase between the AGB and PN stages, PPN are expected to inherit many of the properties of the AGB progenitors. Specifically, many of the observational characteristics of the circumstellar envelopes of AGB stars as the result of mass loss on the AGB are expected to be present in PPN (Kwok 1982). The best way to predict the properties of PPN is to interpolate between the properties of evolved AGB stars and very young PNs. For this reason, it is useful here for us to summarize the properties of these two classes of objects: the progenitors and descendants of PPN.

Observational Properties of AGB Stars

While conventional spectral classification schemes stop at about spectral class M10 for evolved stars, it is now recognized that there exist AGB stars that have evolved beyond this limit. The *IRC*, *AFGL*, and *IRAS* infrared sky surveys have discovered many heavily reddened stars that are redder than Mira variables and are likely to be extremely evolved AGB stars. The circumstellar properties of these stars have been extensively studied in both the infrared and millimeter wave bands.

INFRARED CONTINUUM As a result of mass loss, evolved AGB stars are often obscured by their dusty circumstellar envelopes. As the star ascends the AGB, its mass loss rate increases, and the optical depth of its circumstellar envelope increases. The absorption of photospheric visible photons and the reemission of the energy in the infrared lead to a star of redder color, or lower color temperature.

Oxygen-rich stars (those that have a photospheric O/C abundance ratio greater than 1) are characterized by the 9.7 and 18 μm circumstellar silicate features. The 9.7 μm features changes from emission in early AGB stars (e.g. Mira variables) to self absorption in evolved AGB stars (e.g. OH/IR stars, see Figure 2). As a result of the *IRAS* Low Resolution Spectrometer (LRS) sky survey, more than 3000 oxygen-rich AGB stars have been identified (Volk & Kwok 1987). The evolution of the silicate feature from

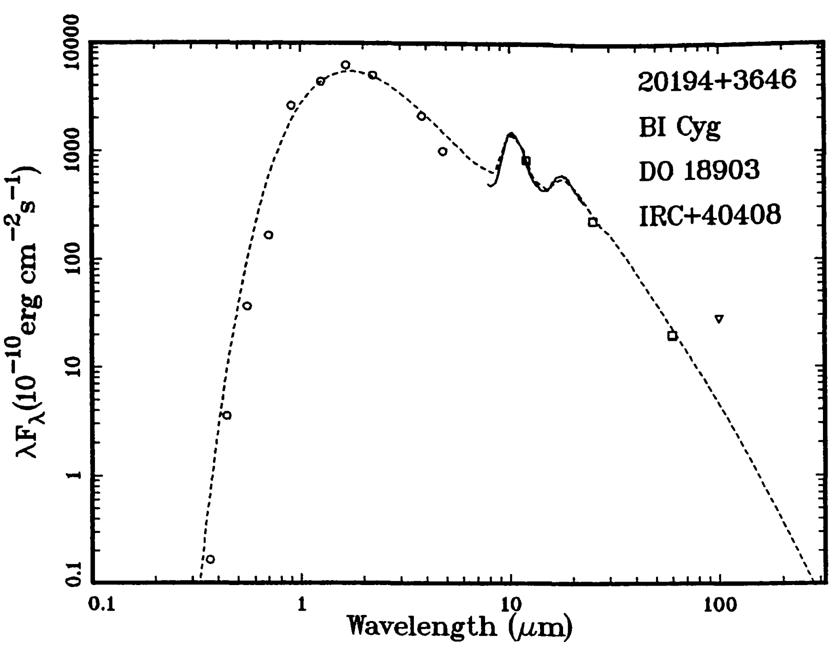

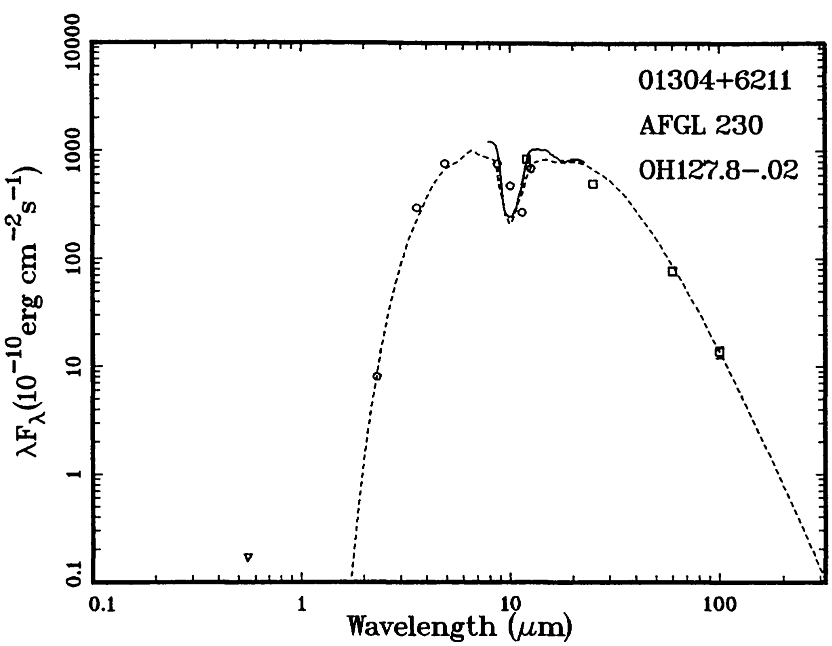

Figure 2 Energy distributions of two oxygen-rich AGB stars. The squares are *IRAS* photometry and the circles are ground-based photometry. Upper limits are indicated by inverted triangles. The dotted lines show fits with a radiative transfer model. The optical depths at 10 μm are 1.5 for BI Cyg and 20 for AFGL 230. The transition from silicate emission to absorption occurs at $\tau \sim 4$.

emission to absorption has been modeled by a radiative transfer model incorporating an increasing mass loss rate as the star ascends the AGB (Bedijn 1987, Volk & Kwok 1988). Figure 3 shows the distributions of AGB stars with silicate emission and absorption features in the *IRAS* color-color diagram. We can see that these oxygen-rich stars form a continuous band in the color-color diagram, which can be explained by a superposition of evolutionary tracks corresponding to stars of different masses. Extension of the theoretical tracks beyond the AGB suggests that the tracks will move to the region of the color-color diagram occupied by PNs.

Evolved carbon stars are characterized by low-color-temperature continua ($T_c \sim$ 500–1000 K) and the presence of the 11.3 μm SiC emission

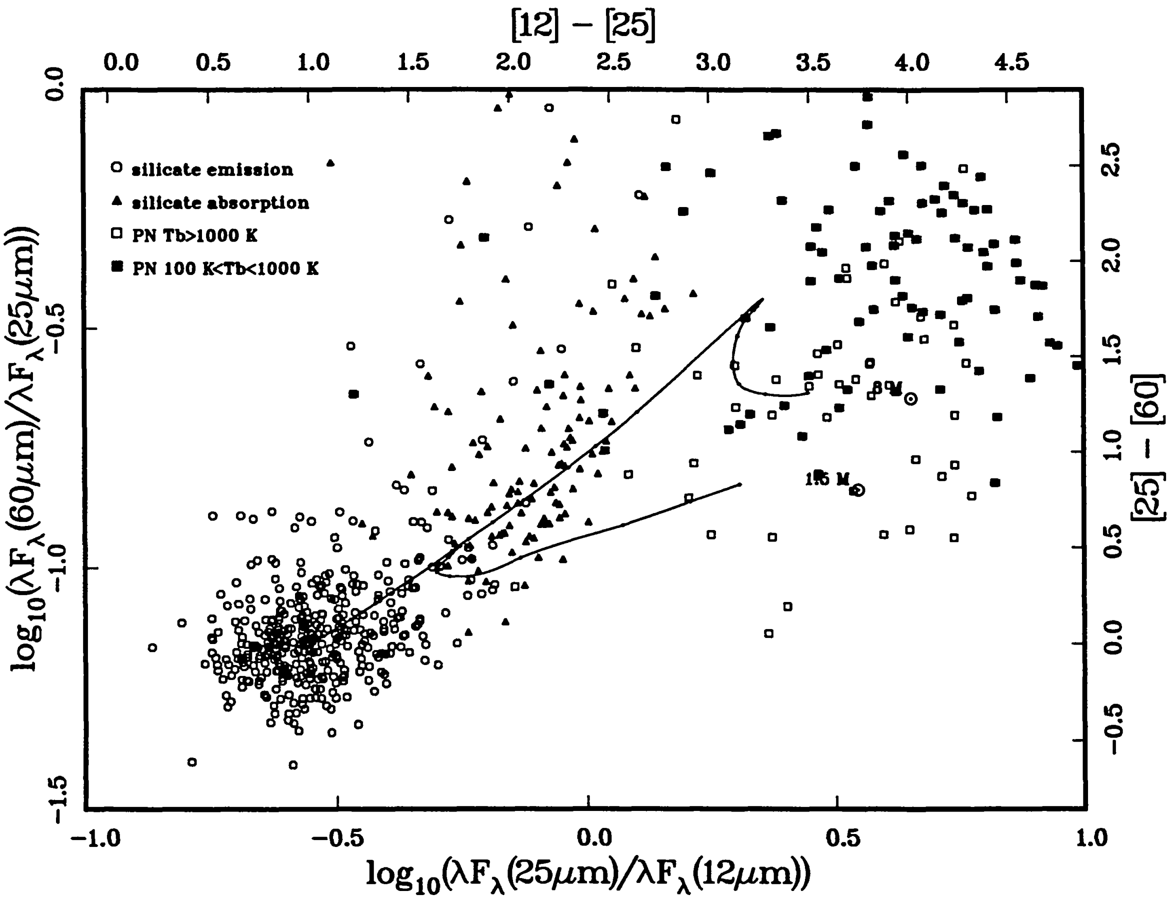

Figure 3 The distribution of AGB stars and planetary nebulae in the color-color diagram. The filled circles are AGB stars showing the silicate feature in emission, and the triangles are AGB stars showing the silicate feature in absorption. The open squares are PNs with 5 GHz brightness temperature (T_b) > 1000 K, and the filled squares are PNs with 1000 K > T_b > 100 K. Also plotted are two PPN evolutionary tracks (for main sequence masses of 1.5 and 8 $M_\odot$ respectively) from Volk & Kwok (1988).

feature (Chan & Kwok 1990). For extremely evolved carbon stars, the color temperature can be as low as 300 K, and these stars generally show a featureless continuum probably due to graphite (Volk et al 1992). The observed energy distributions of evolved carbon stars can be explained by mass loss rates between 10^{-6} and a few times 10^{-5} $M_{\odot}$ yr^{-1}, and their distribution on the *IRAS* color-color diagram can be understood as the result of increasing mass loss rate on the AGB.

MOLECULAR EMISSION Many oxygen-rich AGB stars show double-peaked OH emission profiles, implying an expanding circumstellar envelope. They are historically referred to as OH/IR stars. The OH envelopes can be resolved with radio interferometric techniques; some show bipolar geometries (Bowers 1990). The numbers of OH/IR stars have greatly increased as a result of OH surveys of cool *IRAS* sources (Lewis et al 1985, te Lintel Hekkert 1990).

Since CO is the most abundant molecule (after hydrogen) in the atmospheres of late-type stars, the rotational lines of CO are commonly observed in the circumstellar spectra of both oxygen- and carbon-rich AGB stars (Knapp et al 1982). However, the lines are generally stronger in carbon-rich objects. The CO lines are usually optically thick and have flattop profiles. The estimated mass loss rates for some infrared carbon stars exceed 10^{-5} $M_{\odot}$ yr^{-1} (Knapp & Morris 1985). Several visual carbon stars have also been detected with double-peaked CO emission profiles, which is consistent with the presence of a molecular shell detached from the photosphere (Olofsson et al 1988).

Many infrared carbon stars have rich molecular spectra. For example, in the case of CW Leo, ~30 molecular species have been observed (Olofsson 1987), including organic molecules with molecular weights as high as 147 ($HC_{11}N$). This suggests that complex interstellar molecules could have been synthesized in cool star atmospheres. While the detection of complex molecules has so far been restricted to linear molecules, there is no doubt that other complex molecular species are also present in the circumstellar envelopes of carbon stars. They have just not been detected because their line strengths are diluted by the complexity of their rotational energy structure.

Properties of Young Planetary Nebulae

We define a young PN as a PN with high nebular density and surface brightness, implying a short dynamical age of ~10^3 yr. We should note that since the evolutionary time for the central star to cross the H-R diagram is highly dependent on the core mass (Renzini 1982), a PN with a short dynamical (nebular) age can have an evolved (i.e. high temperature) central star. It is more likely for a young PN to preserve the remnant of the AGB envelope; a more evolved PN would probably have its molecules destroyed by uv radiation, and the dust component diluted by expansion.

INFRARED CONTINUUM Because the evolutionary time from the AGB to the PN phase is short, we expect that the remnant of the circumstellar envelope created during the AGB should still be present in a PN. It has been suggested by Kwok (1982) that many of the circumstellar properties of AGB stars should still be observable in a PN. While infrared excesses have been observed in a number of PNs since as early as 1967 (in NGC 7027; Gillet et al 1967, Cohen & Barlow 1974, Moseley 1980), the origin of the excess has remained controversial for almost two decades. The *IRAS* sky survey provided the first systematic observations of PNs in the far infrared, and a majority of PNs in the Catalogue of Perek & Kohoutek (1967) were detected by *IRAS* (Preite-Martinez 1989). The *IRAS* data for 90 nebulae were analyzed by Pottasch et al (1984) and Iyengar (1986) who found that the color temperatures of the nebulae decrease with increasing radius. An analysis of the energy distribution of young PN shows that the infrared emission from a PN can be separated into two components: a dust component from 10–100 μm, and a nebular (gas) component from 1–10 μm (Kwok et al 1986, Zhang & Kwok 1991). The dust component is clearly the result of the detached dust envelopes of their AGB progenitors. An example of the energy distribution of a young PN is shown in Figure 4.

In Figure 3, we have plotted two groups of PNs in the *IRAS* color-color diagram. We can see that the younger group (defined as those with the highest surface brightness, specifically, $T_b > 1000$ K) in general have higher dust color temperatures than the older group (100 K $< T_b <$ 1000 K). This decrease in color temperature with age can be explained as the consequence of the gradual dispersal of the dust envelope (Kwok 1990).

INFRARED DUST FEATURES While the cooling of the dust component in PNs can seriously weaken the mid-infrared features (such as the 9.7 μm of silicates) since they fall on the exponential side of the Planck function when the dust temperature is below $\sim$100 K (Kwok 1980), both the 9.7 μm feature of silicates and the 11.3 μm of SiC have been detected in a number of young PNs (Aitken et al 1979, Aitken & Roche 1982). The 18 μm silicate feature is also detected by the *IRAS* LRS (Zhang & Kwok 1990, Volk & Cohen 1990). These detections have allowed us to determine directly whether the AGB progenitors of the PNs are oxygen or carbon rich.

However, there exists a family of new infrared features at 3.3, 6.2, 7.7, and 11.3 μm that are not observed in late-type stars. These new features are generally attributed to aromatic hydrocarbons (Duley & Williams

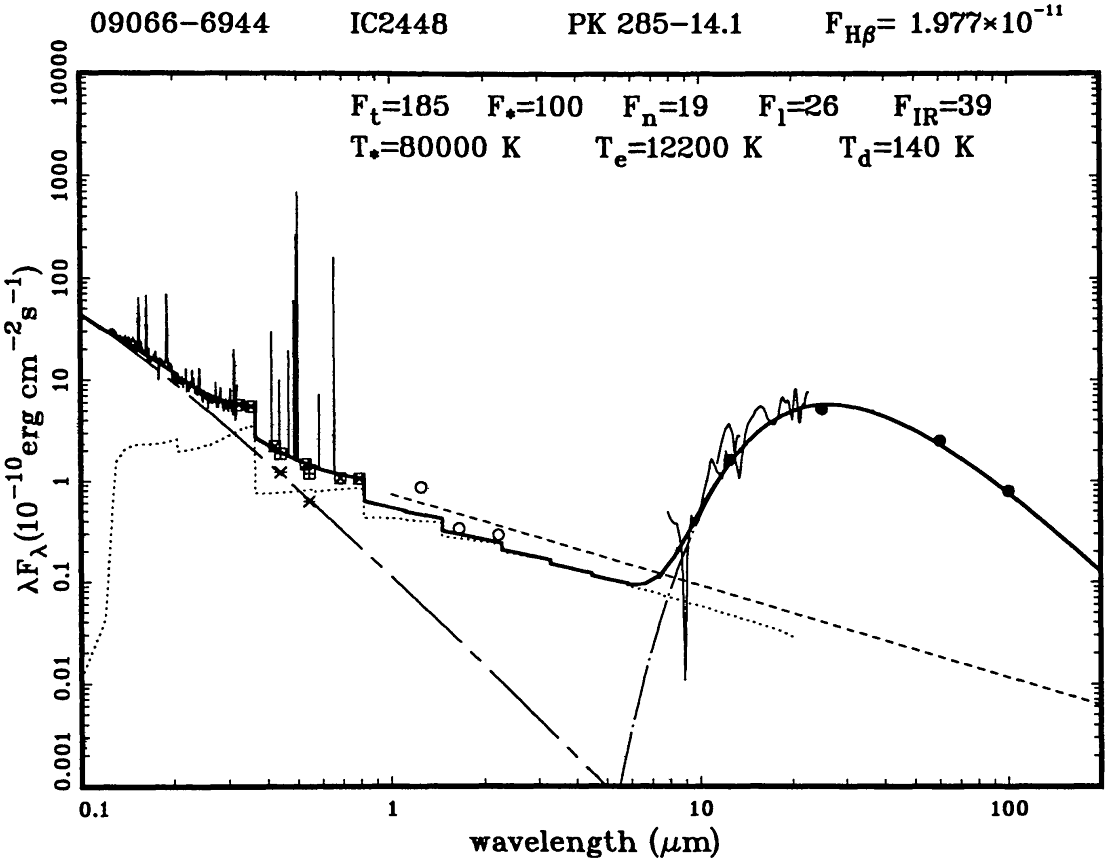

Figure 4 The spectral energy distribution of young PN IC 2448. The dotted line shows the model nebular (b-f and f-f) continuum, the dashed line is the f-f continuum extrapolated from radio measurements, the dot-dashed line is the central star. The total model curve is shown as a solid line. The various symbols are ground-based and *IRAS* observations (from Zhang & Kwok 1991).

1981), and frequently to polycyclic aromatic hydrocarbons (PAH; Léger & Puget 1984). These features are particularly prominent in young carbon-rich PNs with late Wolf-Rayet spectral type (WC12) central stars and large infrared excesses. Some of the examples of such objects are listed in Table 1.

MOLECULAR LINES CO was first detected in the young PN NGC 7027 (Mufson et al 1975) and several other PNs have since been detected (Huggins & Healy 1989; Bachiller et al 1989, 1992). The strength of the CO line is particularly strong in PNs that are high in dust content (e.g. IRAS 21282+5050), suggesting that the dust may have shielded the CO molecule from photodissociation. Since the optical depth of the dust envelope decreases as it disperses into the interstellar medium, the fraction of infrared emission to total observed flux is expected to be highest in young PNs,

Table 1 Planetary nebulae with [WC 11] nuclei and large infrared excesses

IRAS	Other name	IR features (μm)	Molecules
04215+6000	M4-18	8.6[a], 11.3[a]	...
07027-7934	Vo 1[b]	7.7[c], 11.3[d]	CO[e], OH[f]
14562-5406	He2-113	3,3[g], 7.7[d], 8.6[h], 11.3[h]	...
17047-5650	CPD-56°8032	3.3[g], 7.7[i],11.3[h]	CO[e]
17514-1555	...	...	...
21282+5050	...	3.3[j], 7.7[j], 8.6[j,k], 11.3[j,k]	CO[l], HCO^+

[a] Aitken & Roche 1984, [b] Volk & Cohen 1990, [c] Jourdain de Muizon et al 1990, [d] Cohen et al 1985, [e] Loup et al 1990, [f] Zijlstra et al 1991, [g] Allen et al 1982, [h] Aitken et al 1980, [i] Cohen et al 1989, [j] de Muizon et al 1986, [k] Roche et al 1991, [l] Likkel et al 1988.

and to gradually decrease with age. Using a sample of 66 young PNs, Zhang & Kwok (1991) estimate that this fraction is ~1/3. However, for PNs with high mass central stars (e.g. NGC 7027), the central star will evolve so fast that the PN will be ionized even when the dynamical age of the nebula is very young. Such PNs will have an even larger fraction of their total flux emitted in the infrared, and will have the greatest likelihood of maintaining an intact CO envelope.

The OH connection to a PN was first established by the detection of OH in Vy 2-2 (Davis et al 1979), a young oxygen-rich PN showing the 9.7 μm silicate feature. In contrast to the double-peaked profiles commonly found in AGB stars, the OH profile of Vy 2-2 has only the blue-shifted component; the red-shifted component is absorbed by the intervening ionized gas. Since this first detection, several OH-PN associations have been suggested (Zijlstra et al 1989b), but the number of firm detections of OH in PNs remains very low.

RADIO MORPHOLOGY Recent high resolution radio surveys of PNs have revealed that most show "bipolar" morphologies with two brightness peaks (Aaquist & Kwok 1990, 1991; Zijlstra et al 1989a). De-projection models suggest that such morphologies are consistent with incomplete shells formed under the interacting winds mechanism with an asymmetric AGB wind (Volk & Leahy 1992).

Expected Properties of PPN

From the *IRAS* color-color diagrams of late AGB stars and young PNs (Figure 3) we can see that the colors of the two kinds of objects are clearly separated. In fact, a general trend of decreasing color temperature can be observed starting from silicate emission objects, to silicate absorption objects, to PNs with high surface brightness, to PNs with low surface brightness. This apparent evolutionary sequence in the *IRAS* color-color diagram is the result of the monotonic decrease of the dust temperature from the AGB to the PN phase. On the AGB, where the mass loss rate is increasing, the change to lower color temperatures is the result of increasing optical depth in the dust circumstellar envelope. After mass loss has terminated, the decrease in color temperature is caused by geometric dilution as a consequence of the remnant envelope expanding away from the star (Kwok 1990).

Using this empirical color sequence, it is possible to predict the *IRAS* colors of transition objects between AGB and PN phases. Boxes can be drawn in the *IRAS* color-color diagram to search for candidates for PPN (Volk & Kwok 1989, van der Veen et al 1989b, Slijkhuis 1992). Generally speaking, we expect the color temperature of PPN to be in the range of 150–300 K.

SEARCH FOR PPN

Approximately 1000 PNs were detected in the *IRAS* survey. According to the evolutionary models of Schönberner (1983), the fraction of time spent in the PPN phase in relation to the entire PN lifetime is ~10%. If this is the case, we expect ~100 PPN in the *IRAS* Point Source Catalog. These candidates can be identified in two ways: either by looking for stars in existing optical catalogs with appropriate *IRAS* colors, or by searching for the optical couterparts of low-temperature *IRAS* sources. The PPN candidates discovered to date have been found through both of these two strategies.

PPN Candidates Associated with Known Optical Stars

The first attempt to search the *IRAS* Point Source Catalog for associations with G-type stars was by Odenwald (1986). He found that among the 150 G supergiants detected by *IRAS*, excess emission was present in ~4%. Several of the supergiants that he identified are RV Tauri variables, which have long been known to possess infrared excesses at 10 μm (Gehrz 1972). The evolutionary status of RV Tauri stars as post-AGB objects of low mass has been discussed by Jura (1986). A systematic identification of 25 μm-peaking *IRAS* sources with objects for which existing optical spectra are available has been carried out by Bidelman (1985, 1986). Bidelman's extensive list contains several stars of intermediate spectral types (F–K) with large infrared excesses which might be candidates for PPN. A list of

B–G SAO stars with infrared excesses has been compiled by Oudmaijer et al (1992). It is possible that there are post-AGB stars in this list.

High Galactic Latitude Post-AGB Stars

It has been known for some time that a number of high-latitude F supergiants can be better explained as old, halo objects observed in the post-AGB phase rather than young, high mass objects (Bond et al 1984). Among the properties exhibited by various members of this class (but not by all) are high space velocity, low metal abundance (Bond & Luck 1987), circumstellar dust (Parthasarathy & Pottasch 1986), and molecular envelopes (Likkel et al 1987). The supergiant spectral classification reflects the low surface gravity of these stars, but not their intrinsic luminosity. The prototype of this class is 89 Her, which is a MK spectral standard of type F2 Ia. 89 Her is located at a galactic latitude of 23°, which puts it at an unreasonably large distance above the plane if it has the luminosity of a Population I supergiant. Additional support for its post-AGB status comes from its infrared excess (Gillett et al 1970), which could have originated from the remnant of the circumstellar envelope of its AGB progenitor. 89 Her also shows small-amplitude photometric variations (Fernie 1981), suggesting a pulsational period of $\sim$67 days. Velocity variations consistent with a binary period of 278 days have also been observed (Arellano Ferro 1984).

Examples of high latitude luminous stars that have been suggested as post-AGB objects, based on their infrared excesses, include HD 161796 (IRAS 17436+5003, F3 Ib, $b = 30^\circ.9$) and HD 101584 (IRAS 11385−5517, F0 Iep, $b = 6^\circ.0$) by Parthasarathy & Pottasch (1986), HR 4049 (IRAS 10158−2844, B9.5 Ib-II, $b = +22^\circ.9$) by Lamers et al (1986), HD 213985 (IRAS 22327−1731 A2 Ib, $b = -57^\circ$) by Waelkens et al (1987), IRAS 20056+1834 (G0 I, $b = -7^\circ.5$) by Menzies & Whitelock (1988), and IRAS 18095+2704 (F3 Ib, $b = +20^\circ.2$) by Hrivnak et al (1988). The fact that some high galactic latitude supergiants (e.g. IRAS 18095+2704) are too faint to be included in existing optical catalogs suggests that many other as yet-undetected fainter objects of similar nature probably exist.

Two other classes of variable stars are also likely to be post-AGB stars. RV Tauri stars are characterized by light curves showing alternate deep and shallow minima, with periods of 50–150 days, and have spectral type F, G, or K (Preston et al 1963). The circumstellar envelopes of RV Tauri stars can also be seen in CO (Bujarrabal et al 1988, Alcolea & Bujarrabal 1991). The class of UU Her stars is described by Sasselov (1984) as small-amplitude variable stars of periods 40–100 days which are located at high galactic latitudes. Infrared excesses similar to 89 Her have been found in

RV Tauri (Gehrz 1972), but not in UU Her (Gehrz & Woolf 1970). A comprehensive study of 25 high galactic latitude supergiants with infrared excesses was made by Trams (1991).

A number of high latitude supergiants (e.g. HR 4049) have been found to be extremely metal deficient and such metal depletion could be the result of mass transfer in a binary system or re-accretion of the gas component in the outflow (Mathis & Lamers 1992, Trams et al 1992, Waters et al 1992).

There are a number of other peculiar infrared sources that have been suggested as stars in the post-AGB phase of evolution. The most well-known examples are the HD 44179 (the red rectangle, Cohen et al 1975) and the Frosty Leo nebula (IRAS 09371+1212, Forveille et al 1987). HD 44179 is a star of uncertain spectral type between B9 and F which shows strong PAH features (Russell et al 1978). The Frosty Leo nebula has a large far-infrared excess due to the 45 μm ice band (Omont et al 1989). The ice band also shows up as a prominent absorption feature at 3.1 μm (Geballe et al 1988). From the polarization images of the nebula, Dougados et al (1990, 1992) suggest that the expanding dust is in the form of disk seen edge on. From the derived inner radius of the disk, they suggest that it was ejected a few hundred years ago.

R CrB is a G0 Iep supergiant at a galactic latitude of 51°. It is a hydrogen deficient carbon star with large-amplitude variability over time scales of a few years. *IRAS* images show dust shells extending over 18 arc min (Gillett et al 1986), which could represent the remnant envelope ejected in previous mass loss episodes.

Cool IRAS *Sources as PPN Candidates*

The search for PPN candidates by ground-based observations of *IRAS* sources satisfying certain color criteria has been carried out by several groups (Kwok 1987, van der Veen 1988, Hu et al 1992a). Candidates are selected from a certain region of the *IRAS* color-color diagram and are identified with a ground-based telescope or by positional coincidence on sky survey plates. Photometric observations are used to obtain the spectral energy distribution and spectroscopic observations are made to determine the spectral type of the central star. These can also be followed by molecular observations and optical/infrared imaging.

This search strategy for PPN depends critically on the correct identification of the optical counterpart of the *IRAS* source. Many *IRAS* sources are evolved AGB stars which suffer from large circumstellar extinction and thus will not be visually bright (Kwok et al 1987). Association of stars in optical survey plates with the *IRAS* source by pure positional coincidence can easily lead to the wrong identification of the *IRAS* source, in particular in the Galactic plane where the field is crowded. Even when a counterpart is identified by searching in the *K* band, the possibility for confusion still exists because most red stars are strong near-infrared emitters. The only sure way to obtain the correct identification is by searching around the *IRAS* position at 10 or 20 μm, and comparing the observed fluxes with the *IRAS* 12 and 25 μm PSC fluxes. While the *IRAS* positions are generally good, there are cases where the actual source can be up to 1 arc min from the PSC position.

Owing to these uncertainties, it is difficult to evaluate the PPN nature of some of the candidates proposed in the literature. If the visible star is spectroscopically classified as an F or G supergiant (e.g. 18025−3906 in Hu et al 1992a), then the probability of it being a PPN is higher.

In Table 2 we have tabulated 28 objects that we consider to be good candidates for PPN. Two examples of the energy distributions of PPN are shown in Figure 5. The most outstanding characteristics of the energy distributions of these objects is that they show two distinct components, each contributing significantly to the total observed flux. The cooler component corresponds to the remnant of the AGB dust envelope and the warmer component corresponds to the reddened photosphere of the central star. The clear separation of the two components suggests that the dust envelope is detached from the photosphere, consistent with the theoretical expectation that the AGB mass loss has terminated some time ago. The dynamical age (after the cessation of mass loss) of these objects can be estimated by radiative transfer models, and the typical time scales of the PPN in Table 2 range from several hundred years to more than a thousand years (Hrivnak et al 1989).

The PPN list in Table 2 is biased toward stars with large mass loss rates on the AGB. These stars have large infrared excesses and their evolution can be traced from the AGB to PN through infrared observations. Consequently we have higher confidence that they will evolve into PNs. Other post-AGB objects that evolve from AGB stars with lower mass loss rates probably exist (e.g. some of the objects discussed in the previous section) but are not listed in Table 2.

THEORETICAL MODELS

If we assume the infrared spectra of PPN to be dominated by radiation from the remnant of the circumstellar envelope of an AGB progenitor, models for PPN can be constructed by extrapolating the models for AGB stars beyond the AGB. The PPN models should incorporate two aspects of PPN evolution: the dispersion of the circumstellar envelope and the evolution of the central star. A first attempt at PPN evolution was made by Bedijn (1987) who considered nonvariable OH/IR stars as possible

Table 2 Proto-planetary nebulae candidates

IRAS	Other name	Spectral type	l	b	Infrared	Mol. line	Ref.
04296+3429	–	G0 Ia	166.2	−9.1	21 μm	CO	a
04395+3601	AFGL 618	B0	166.5	−6.5	featureless	CO	
05113+1347	–	G8 Ia	188.8	−9.1	21 μm	–	b
05381+1012	–	G	195.5	−10.6	–	–	
06530−0213	–	F0 I	215.4	−0.1	–	CO	c
07134+1005	HD 56126	F5 I	206.7	+10.0	21 μm	CO	a,d
10215−5916	DM−583221	G5: I	285.1	−1.9	silicate	–	d,h
12175−5338	SAO 239853	A9 Iab	298.3	+8.7	–	–	d
17150−3224	–	G2 I	353.8	+3.0	–	OH,CO	c,g,h
17436+5003	HD 161796	F3 Ib	77.1	+30.9	–	OH,CO	d,e
17441−2411	–	–	4.2	+2.2	–	CO	c,h
18025−3906	–	G2 I	353.3	−8.7	–	OH	c
18095+2704	–	F3 Ib	53.8	+20.2	silicate	OH	f,g
19114+0002	HD 179821	G5 Ia	36.6	−5.0	silicate	OH,CO	d,g
19454+2920	–	–	65.2	+2.1	featureless	CO	i
19475+3119	313797	F3 Ia	67.1	+2.7	–	CO	
19477+2401	–	–	60.8	−0.9	–	OH	
19480+2504	–	–	61.8	−0.6	featureless	CO	
19500−1709	HD 187885	F3 I	24.0	−21.0	–	CO	d,g
20000+3239	–	G8 Ia	69.7	+1.2	21 μm	CO	b
20004+2955	V 1027 Cyg	G7 Iab	67.4	−0.4	silicate	–	d,h
20028+3910	–	–	75.5	+4.2	featureless	CO	h
	AFGL 2688	F5 Ia	80.2	−6.5	featureless	CO	
22223+4327	DO 41288	G0 Ia	96.7	−11.5	21 μm	CO	
22272+5435	HD 235858	G5 Ia	103.3	−2.5	21 μm	CO	a,g,k
22574+6609	–	–	112.0	+6.0	21 μm	CO	j
23304+6147	–	G0 Ia	113.9	+0.6	21 μm	CO	a
23321+6545	–	–	115.2	+4.3	–	OH,CO	h

References: (*a*) Kwok et al 1989, (*b*) Kwok et al 1993, (*c*) Slijkhuis 1992, (*d*) Hrivnak et al 1989, (*e*) Parthasarathy & Pottasch 1986, (*f*) Hrivnak et al 1988, (*g*) van der Veen 1988, (*h*) Volk & Kwok 1989, (*i*) Kwok et al 1987, (*j*) Hrivnak & Kwok 1991b, (*k*) Pottasch & Parthasarathy 1988.

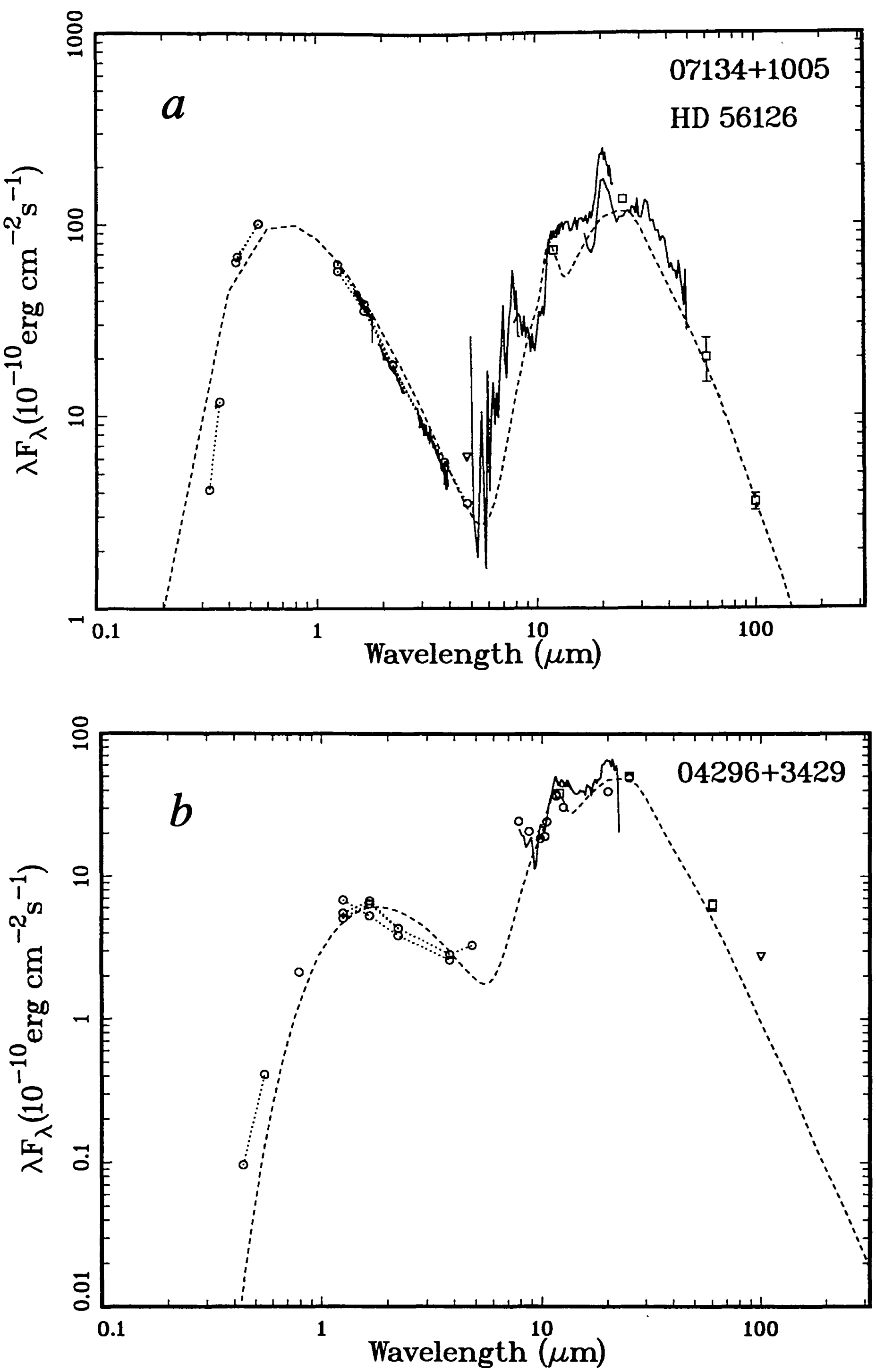

Figure 5 Spectral energy distribution of two PPN candidates. The symbols are the same as Figure 2. (*a*) 07134+1005: The H, K, and L spectra are from Kwok et al (1990), the 5–8 μm spectrum is from Buss et al (1990), and the 30–60 μm spectrum is from Omont et al. (1993). (*b*) 04296+3429.

candidates for PPN. A similar model using a different AGB mass loss formula was calculated by Volk & Kwok (1988), and their results have been used to fit the energy distributions of a number of PPN candidates (Volk & Kwok 1989). In all of these models the central star is assumed to be static. Recently, Volk (1992) and Marten et al (1993) have calculated more realistic nebular evolution models of PPN using respectively the central star evolution models of Schönberner (1983) and Blöcker (1989). A variety of mass loss rates at the end of the AGB were used to determine the dust emission spectrum at different times beyond the AGB. Tracks on the *IRAS* color-color diagram are also calculated by convolving the *IRAS* bandpasses with the model spectra. Marten et al (1993) include the effects of grain-gas coupling in their dynamical calculations and find that it has great influence on the PPN tracks in the *IRAS* color-color diagram. In order to obtain agreement with the observations, Volk (1992) found that the Schönberner (1983) tracks have to be speeded up and that the PPN phase cannot exceed $\sim$800 yr. The spectral evolution of a star with a relatively high rate of mass loss is shown in Figure 6. We can see that the energy distributions of both young PNs (Figure 4) and PPN (Figure 5) can be reproduced successfully in this model.

OPTICAL PROPERTIES OF PPN

The PPN candidates in Table 2 vary greatly in apparent magnitude, ranging from $\sim$7 mag to $>$22 mag. For the optically bright objects, spectroscopic studies are possible. For the faint objects, visible photometry has been obtained for most of them.

Many PPN candidates (in particular those of spectral type FI) show emission activity in Hα. The Hα profiles range from P Cygni, inverse P-Cygni, to shell (Waters et al 1993). Such profiles are also observed in a few yellow supergiants (Sowell 1990), and in pulsating stars such as the RV Tauri and W Vir stars. The variations in Hα suggest that the stars may be losing mass in an episodic manner and have wind velocities of 100–300 km s^{-1} (Waters et al 1993).

Velocity monitoring of a number of PPN candidates has produced several binary candidates (Waters et al 1993, Hrivnak & Woodsworth 1993). At this point, it is too early to say what fraction of the PPN candidates are in binary systems. Additional velocity measurements over the next few years will be needed to settle this question.

Visual observations of some optically bright post-AGB stars (e.g. RV Tauri stars) have been made for over a century, and pulsational period changes are detectable. The period changes of two RV Tauri stars are

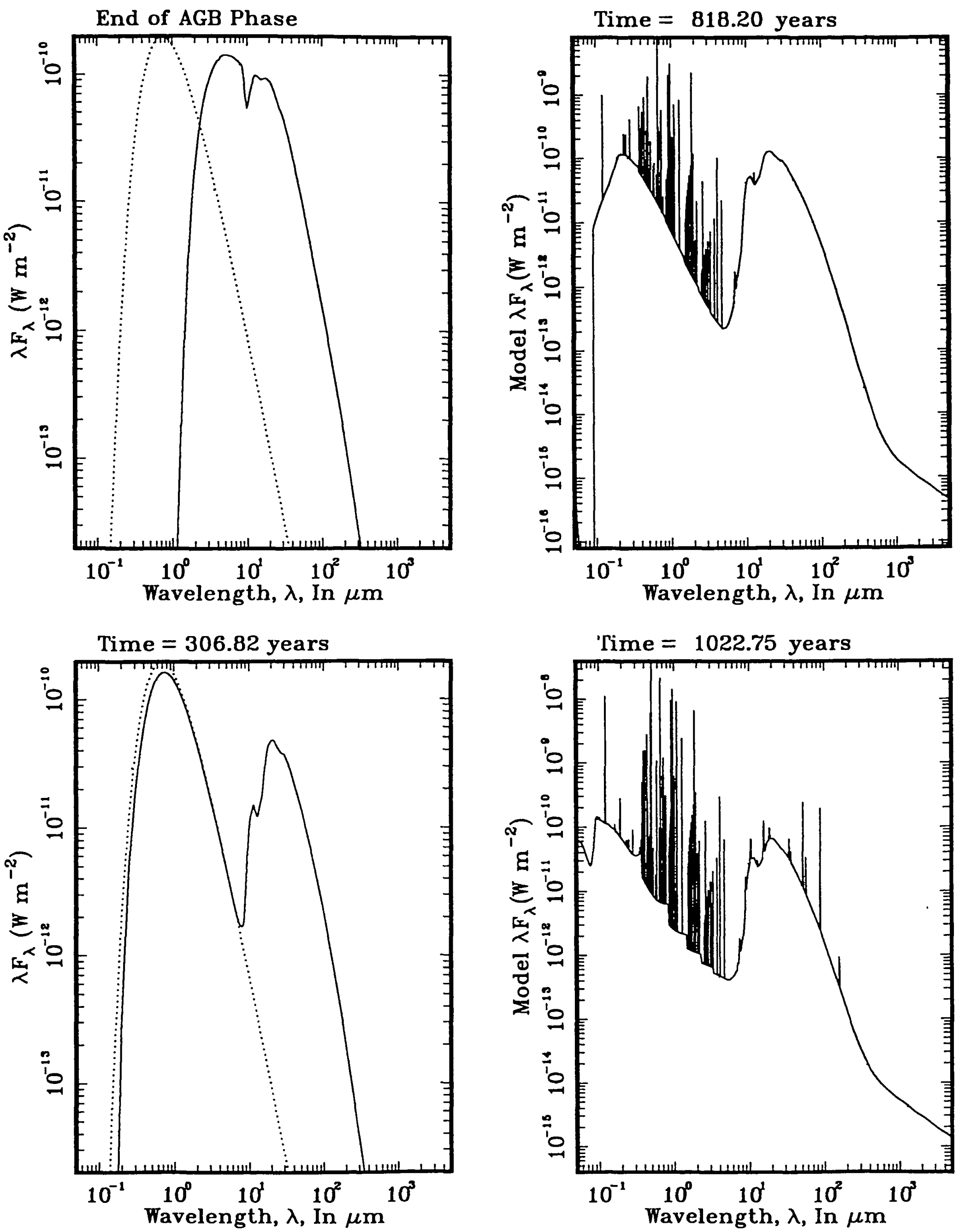

Figure 6 Spectral evolution from the end of AGB (*top left*) to PPN (*bottom left*), to PN (*bottom right*). The solid lines show the emergent spectra and the dotted lines in the left panels show the blackbody spectra of the embedded stars. The model assumes that the circumstellar dust shell detaches from the photosphere at the end of the AGB, and the central star evolves according to the 0.64 $M_{\odot}$ track of Schönberner (1983). The 10 μm optical depth is 20 at the time of shell detachment. These models are from Volk (1992).

found to be consistent with the expected period evolution of post-AGB stars (Percy et al 1991).

Molecular bands of C_2 and C_3 have been detected in AFGL 2688 (Crampton et al 1975) and a few other PPN (Hrivnak & Kwok 1991b), suggesting that these are highly carbon-rich objects.

INFRARED PROPERTIES OF PPN

Continuum Properties

The infrared continua of PPN candidates are well defined by the combination of *IRAS* photometry at 12, 25, 60, and 100 μm and ground-based near- and mid-infrared photometry. In most cases, the near-infrared arises from the reddened photosphere and while longward of 5 μm the dust component dominates the continuum. The dust component generally is well-fitted by a single temperature blackbody. At longer wavelengths, the dust continuum may deviate from a blackbody as the result of decreasing dust opacity with increasing wavelength. Submillimeter continuum observations can help better define the shape of the dust continuum and even the mass loss history (van der Veen et al 1992).

The infrared continua of PPN candidates are expected to have color temperatures of 150–300 K, i.e. between the color temperatures of the most evolved AGB star and the youngest PN. However, the continuum properties alone cannot define a proto-planetary nebula, for young (or proto-) stars are also expected to have similar color temperatures. It has been argued that if there is significant mass loss in the post-AGB stage, hot dust in the form of near-infrared excess would also be seen (Trams et al 1989). HR 4049 can be considered as a prototype of these objects. Some PNs (e.g. NGC 7027: Russell et al 1977; IC 418: Zhang & Kwok 1992) are known to have a hot dust component in addition to a cool dust component from the AGB mass loss, so it is possible that some post-AGB objects will show near-infrared excess as well.

Circumstellar Dust Features

OXYGEN-RICH PPN: SILICATES Since the 10 and 18 μm features of silicates are commonly observed in oxygen-rich AGB stars, it is expected that these features will also be observable in oxygen-rich PPN. It has been noted that the 10 μm feature in PPN will be much less prominent than in AGB stars because of the decline in dust temperature and the shift of the spectral peak to longer wavelengths (Kwok 1980). This effect is quantitatively confirmed by the detached-shell radiative-transfer model of Volk & Kwok (1989) who find that the 10 μm feature not only weakens but also broadens. A search of the *IRAS* LRS has yielded a number of sources with the predicted shape at 10 μm (Volk & Kwok 1989). A number of these objects have now been confirmed to be PPN (e.g. 18095+2704, 10215−5916, and 20004+2955). The existence of oxygen-rich PPN confirms the evolutionary connection between OH/IR stars and PNs.

CARBON-RICH PPN *The 21 μm feature* The dominant circumstellar dust grains in carbon-rich AGB stars are SiC and (in extreme carbon stars) graphite. The strength of the 11.3 μm SiC feature is weaker than the 10 μm silicate feature, and graphite is featureless in the mid-infrared. These facts have led us to assume that carbon-rich PPN will not have strong identifying features in the 10–20 μm range. The discovery of a strong emission feature at 21 μm in four PPN therefore came as a surprise (Kwok et al 1989). The *IRAS* LRS of these four sources show a prominent feature at 21 μm with an almost flat (in λF_λ) continuum between 12 and 18 μm (Figure 7). The 21 μm feature has been confirmed by both airborne (Omont

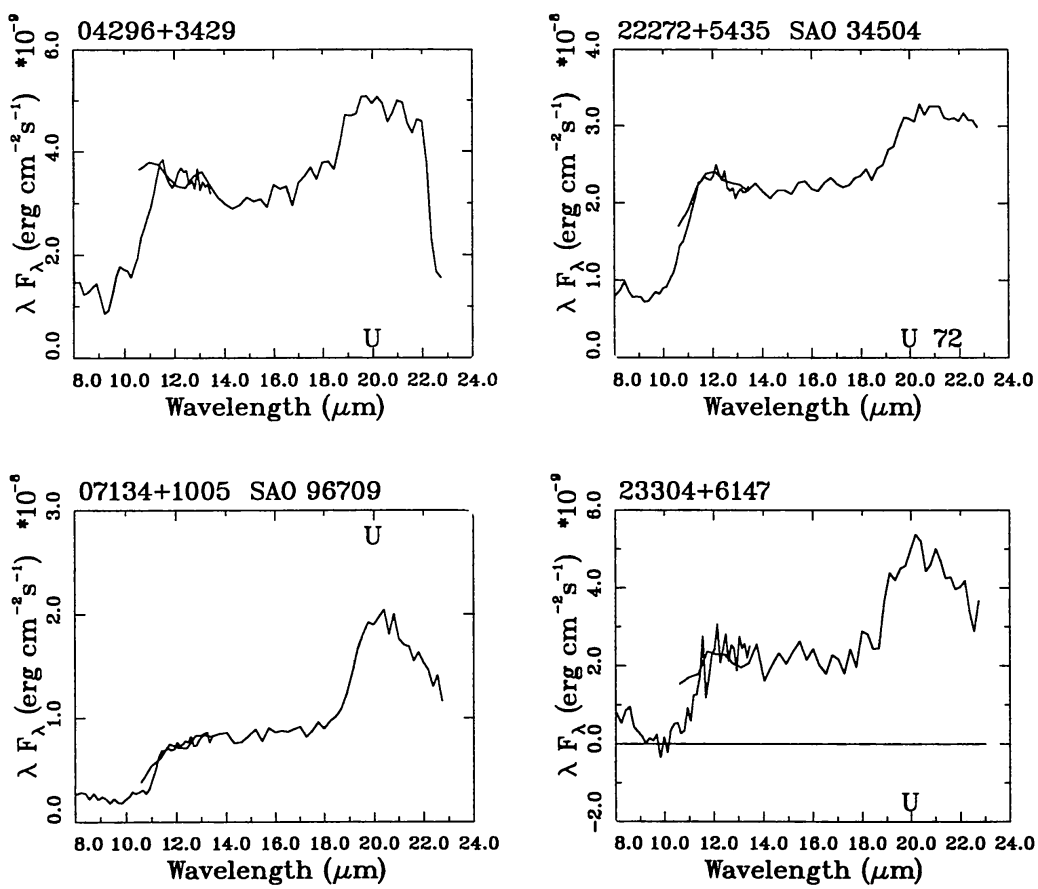

Figure 7 The LRS spectra of four PPN showing the 21 μm feature. For explanation of the LRS letter classification codes see Volk et al (1991).

et al 1993) and ground-based observations (Barlow 1993). This feature has not been seen in the spectrum of AGB stars or PNs, but only in PPN.

Several suggestions have been made about possible origins of this feature. Cox (1990) found similar features in a number of HII regions, and proposes that the feature is due to Fe_2O_3 or Fe_3O_4. Sourisseau et al (1992) suggest that the 21 μm feature arises from a mixture of coal, SiC, and urea. The strength of the 21 μm feature implies that it originates from abundant atomic species. The fact that it is associated with carbon-rich objects suggests that carbon may be a major constituent. The wavelength and strength of the feature suggest that it is due to a vibrational band in a highly symmetric molecule.

3.3 and 6.9 μm features In addition to the well-known 3.3 μm PAH emission feature that is commonly observed in PN and HII regions, there exist emission features in the 3.4–3.5 μm region which, although present in PNs, are found to be strongest in PPN. These features have been detected in the PPN candidates 05341+0852 (Geballe & van der Veen 1990), 04296+3429, 22272+5435 and AFGL 2688 (Geballe et al 1992), as well as the C-rich PN 21282+5050 (Geballe & van der Veen 1990). Several identifications have been proposed for the carriers of the 3.4–3.6 μm emission features. Barker et al (1987) and Allamandola et al (1989) have suggested that the 3.46, 3.51, and 3.56 μm features are hot bands of the fundamental C-H vibrational stretch at 3.29 μm in PAHs. de Muizon et al (1986) and Jourdain de Muizon et al (1990) propose that these and other weak features are the fundamental C-H stretches of side-groups of PAHs. They also have suggested that overtones and combinations of C–C vibrations may be responsible for the underlying plateau.

Airborne observations of two of these 21 μm sources (07134+1005 and 22272+5435) in the 5–8 μm region showed that the 6.9 and 8 μm features are also present in these PPN (Buss et al 1990). These features closely resemble the unidentified emission bands observed in HII regions and PNs. While the 3.3 and 6.2 μm features observed in HII regions and PNs are thought to be fluorescently excited by UV photons, this cannot be the case in these PPN because of their late spectral types. If these bands in PPN are excited by visible photons, then the molecules responsible must be larger (>100 C atoms) than interstellar PAH molecules (Buss et al 1990). Based on the strength correlation between the 3.4–3.5 μm features and the 6.9 μm feature in 22272+5435, Geballe et al (1992) suggest that the former is due to the stretching mode of CH_2 and CH_3 groups. Because of the different temperatures of the exciting stars in PNs and PPN, the strengths of the 3.4–3.5 μm relative to the 3.3 μm features are due to the different amount of UV and visible photons available.

Atomic and Molecular Lines

The near-infrared spectrum of PPN candidates, in particular those of F spectral type, are dominated by hydrogen recombination lines in absorption (Figure 8*a*). For objects of later spectral type (mid-G or later), vibrational bands of CO are generally seen in absorption (Figure 8*b*), although in several cases these bands are in emission. The most interesting case is 22272+5435 for which the CO spectrum has been seen to change from emission to absorption over a three month interval (Hrivnak et al 1993).

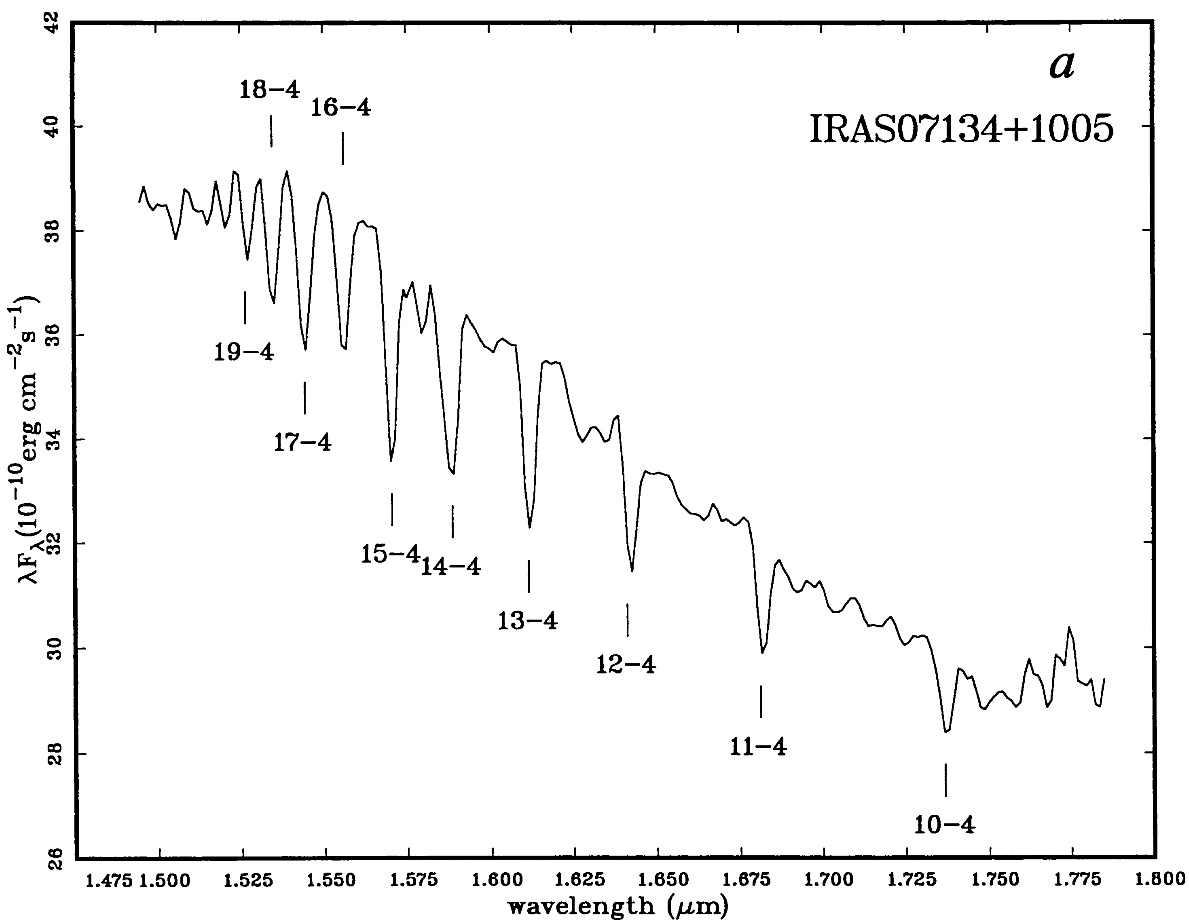

Figure 8 (*a*) H band spectrum of 07134+1005 showing ten hydrogen Brackett lines in absorption. The lines marked with *x* are spurious features introduced by absorption features in the reference spectrum. (*b*) K band spectrum of 20000+3239 showing the CO bands (v = 2–0 to 8–6) in absorption. The 7–4 line is a recombination line of hydrogen.

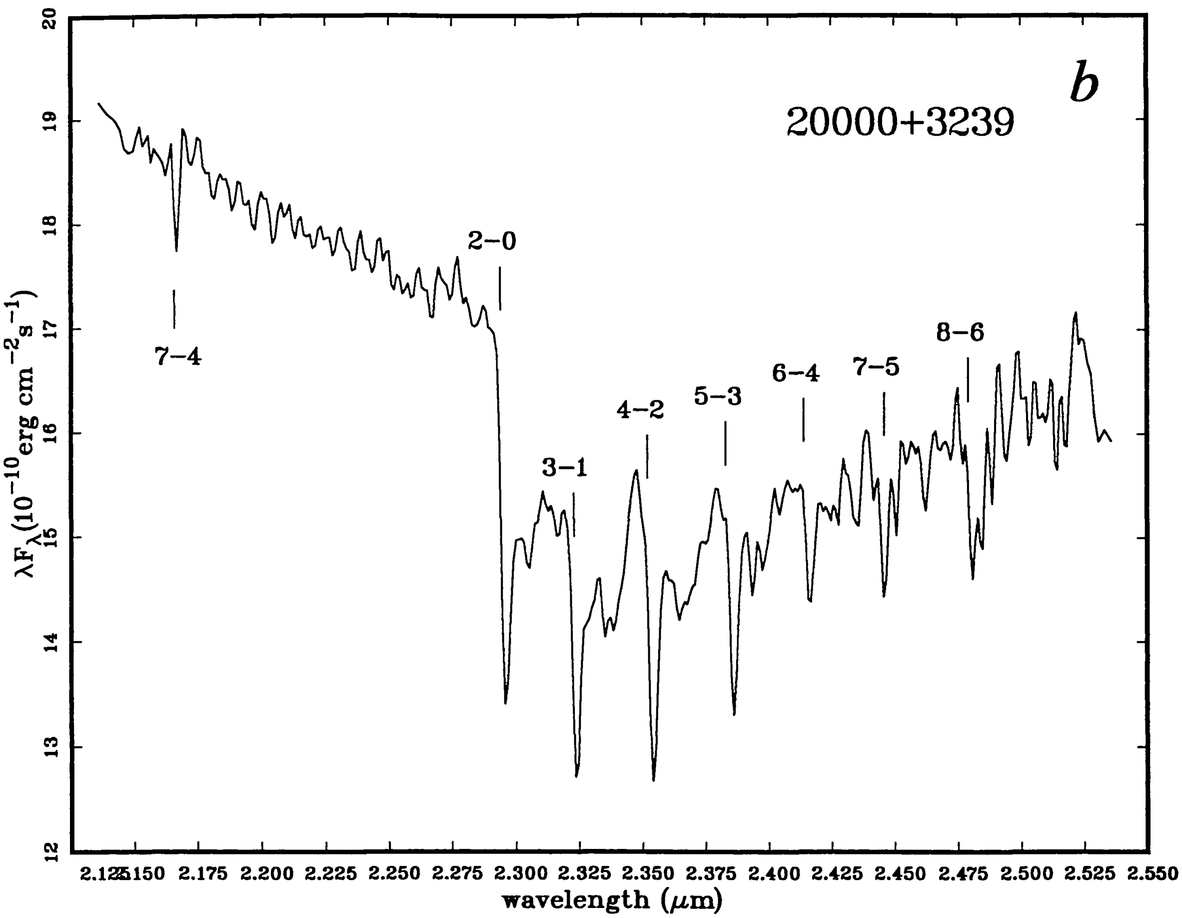

Figure 8 (*continued*).

CIRCUMSTELLAR MOLECULAR EMISSIONS

OH Maser Emission

While oxygen-rich AGB stars exhibit maser emissions in OH, H_2O, and SiO, not all of these emissions are expected to persist through the PPN stage. Theoretical calculations by Sun & Kwok (1987) suggest that only stars with high mass loss rates will have 1612 MHz emission that is detectable through the PPN stage. An evolutionary scenario of how the strengths of these maser lines will vary after the star has left the AGB is outlined by Lewis (1989). For example, the proto-planetary nebula IRAS 18095+2704 shows OH main (1665/1667 MHz) lines that are stronger than its 1612 MHz line—the opposite of what is usual in AGB stars (Lewis et al 1990). An OH and H_2O survey of cool *IRAS* sources by Likkel (1989) has detected several PPN candidates (17436+5003, 19114+0002, 19477+2401, 23321+6545), all in the main lines.

Of particular interest is the OH 1667 MHz main-line maser emission from the post-AGB star candidate HD 101584 (IRAS 11385−5517). The blue- and red-shifted components are well separated in bipolar lobes on opposite sides of the stellar position (te Lintel Hekkert et al 1992). The measured expansion velocity increases from 9 km s^{-1} at the inner edge of each lobe to 40 km s^{-1} at the outer edge. It is likely that the OH emission occurs along the polar axis of an equatorial disk of circumstellar dust.

CO Thermal Emission

Since the lower rotational transitions of the CO molecule have been detected in the circumstellar envelopes of more than 200 AGB stars (Knapp & Morris 1985), it is expected that CO emission should still be detectable in PPN after the shell has detached from the photosphere. Indeed, the early candidates for PPN (e.g. AFGL 618, AFGL 2688) all show strong CO emission. The detection of CO emission in PNs confirms this connection.

The detection of CO emission in PPN first resulted from general surveys of cool *IRAS* sources. These include the use of the FCRAO 14 m by Arquilla et al (1986); NRAO 12 m by Zuckerman and Dyck (1986a,b); IRAM 30 m by Likkel et al (1987) and Omont et al (1992); and the OSO 20 m and SEST 15 m by Loup et al (1990) and Nyman et al (1992). Later searches which are more specific to known PPN candidates include Woodsworth et al (1990), Likkel et al (1991), Bujarrabal et al (1992), van der Veen et al (1993), and Hu et al (1992c). It is interesting to note that almost all PPN candidates studied have been found to have CO emission (see Table 2). All detected PPN sources show broad profiles (FWHM 20–30 km s^{-1}) typical of AGB stars.

As in AFGL 618 and AFGL 2688, broad extended wings have been detected in the PPN candidate IRAS 19500−1709 (Bujarrabal et al 1992), suggesting a fast velocity outflow during the PPN phase.

The mass loss rates responsible for the creation of the remnant AGB envelope in PPN are generally estimated by applying the formula of Knapp & Morris (1985). Since the energy distributions of the PPN are well determined, the momentum flux (MV) represented by the derived mass loss rates can be compared to the radiative momentum implied by total observed fluxes ($4\pi D^2 F/c$), where D, F, and c are the distance, total flux, and the velocity of light, respectively. The ratio of these two momentum fluxes is generally referred to as β (Knapp 1986). While the values of β for AGB stars are ~ 1, the corresponding values are higher for PPN and highest for PNs (Likkel 1989, Hrivnak & Kwok 1991a).

The CO envelope of IRAS 19114+0002 was found to be partially resolved by Bujarrabal et al (1992). The envelope shows an elongated structure of approximately $18'' \times 14''$. Future millimeter-wave interferometry observations should produce much improved morphologies of the PPN molecular envelopes and therefore allow us to more accurately estimate the fraction of PPN that have nonspherically symmetric envelopes.

Radio Continuum

The detection of a very small ionized region in the proto-planetary nebula AFGL 618 (Kwok & Bignell 1984) and the detection of OH emission in the very young planetary nebula Vy 2-2 (Davis et al 1979) suggest that PPN just about to enter the PN stage could show evidence of a nascent ionized region. The ionized component can be detected by infrared recombination lines (e.g. Br γ) or by f-f emission. A number of OH/IR stars have been searched for radio continuum radiation (Herman et al 1985, Rodriguez et al 1985, Pottasch et al 1987, Bowers & Knapp 1992). The object IRAS 17516−2525 does not show continuum radiation but the detection of Br α, Br γ, and Pf γ suggests that this object could be a proto-planetary nebula in transition to a PN (van der Veen et al 1989a).

MORPHOLOGY

Since two of the early PPN candidates (AFGL 618 and AFGL 2688) show bipolar morphology, there has been a great deal of interest in exploring the relationship between PPN and bipolar nebulae. Hrivnak & Kwok (1991a) found that several PPN have similar spectra in the mid-infrared but have vastly different optical brightnesses. They interpret this difference as the result of PPN with non-spherically-symmetric envelopes being viewed at different orientations. The optically bright ones are likely to be pole-on systems while optically faint ones are edge-on.

Optical Imaging

If the mass loss from the AGB progenitor has not been perfectly spherically symmetric, then scattered light escaping from the poles will result in edge-on systems showing bipolar morphology. PPN candidates found to show bipolar morphology include 17150−3224 and 17441−2411 (Hu et al 1992b, Langill et al 1993).

A high resolution (0.5 arc sec) image of AFGL 2688 has been obtained by Crabtree & Rogers (1993). The image shows a series of concentric rings around the stars with spokes extending as far as 35″ from the star. These rings can be interpreted as events of episodic mass loss at intervals of 600 yr.

Infrared Imaging

While the visible light traces scattered light, the distribution of dust material around the central star can be mapped by infrared imaging. Near-infrared imaging of AFGL 2688 in the H_2 line shows a ring-like structure perpendicular to the visible lobes (Gatley 1988, Smith et al 1990). Recent advances in mid-infrared imaging technology allow the morphology of PPN to be determined by imaging in the major dust features. For example, the observations by Meixner et al (1992) show that the oxygen-rich proto-planetary nebula HD 161796 has a 3 arc sec spherical dust shell whereas the carbon-rich proto-planetary nebula 22272+5435 shows an elongated morphology.

CONCLUSION

Significant progress has been made in the past decade toward the identification of PPN and a general understanding of the post-AGB phase of evolution. A self-consistent evolutionary model to link the AGB and PN phases has been constructed. Candidates that closely resemble the predicted properties of PPN have been found. The evolution of the remnant AGB envelope can be followed throughout this transition phase, giving us confidence that these candidates are likely to evolve into planetary nebulas.

However, a number of problems remain:

1. The relationship between the high latitude supergiants with infrared excesses (e.g. 89 Her) and PPN is not clear. It is possible that the former represent low mass stars that are evolving slowly and have transition times longer than the dynamical lifetime of the nebula. If this is the case, then these stars will never become PNs and they would be more accurately called post-AGB objects rather than PPN. The spectral behavior of low mass stars in the post-AGB phase can be quite different from high mass stars, and such differences have to be investigated further.
2. It is not certain at this point what fraction of the present PPN candidates are in binary systems. The possible effects of mass transfer will certainly complicate the simple-minded picture we have today.
3. Why do some PPN (and for that matter PNs) show bipolar morphology while others do not? How is the nebular shape related to the mass loss process on the AGB? Could there be a difference between oxygen-rich and carbon-rich stars?
4. Is the mass loss history on the AGB steady or episodic? Higher res-

olution imaging of the envelope around PPN will be able to resolve this issue.

5. It may be difficult to identify some post-AGB stars because of their spectral resemblance to young stellar objects. The problem of distinguishing between young and old stars will continue to be a source of confusion. Since high-mass stars also have large mass loss rates while they are red supergiants, it may be difficult to distinguish massive stars that are evolving to blue supergiants (e.g. IRC+10420) from PPN.
6. The infrared spectra of PPN show unique features different from infrared features seen in other celestial sources. Is this difference due to the chemical synthesis process in PPN or is it a manifestation of their excitation conditions?

Looking into the future, we can anticipate the advance from one-dimensional to two-dimensional PPN models. There is evidence that the mass loss in some AGB stars is not spherically symmetric, and such asymmetric structures will have an influence on the dynamical evolution of PPN. High resolution mapping of PPN objects will help us understand the origin of the bipolar structures in many PNs. The beginning of the fast wind in the central star will be better determined, leading to a better realization of its effects on the morphology and evolution of planetary nebulas.

Acknowledgments

I am indebted to Bruce Hrivnak who has collaborated with me on many aspects of PPN research. I would also like to thank my other co-workers Kevin Volk and C. Y. Zhang for their ideas and contributions to this subject. This review would not have been possible without the input and preprints from other researchers in this field, in particular William Bidelman, Thomas Geballe, Goran Sandell, Detlef Schönberner, and Rens Waters. Lorraine Volsky gave a critical reading of an earlier draft of this manuscript. This work is supported by the Natural Sciences and Engineering Research Council of Canada.

Literature Cited

Aaquist, O. B., Kwok, S. 1990. *Astron. Astrophys. Suppl.* 84: 229–58

Aaquist, O. B., Kwok, S. 1991. *Ap. J.* 378: 599–610

Aitken, D. K., Roche, P. F. 1982. *MNRAS* 200: 217–37

Aitken, D. K., Roche, P. F. 1984. *MNRAS* 208: 751–61

Atiken, D. K., Roche, P. F., Spenser, P. M., Jones, B. 1979. *Ap. J.* 233: 925–34

Aitken, D. K., Barlow, M. J., Roche, P. F., Spenser, P. M. 1980. *MNRAS* 192: 679–87

Alcolea, J., Bujarrabal, V. 1991. *Astron. Astrophys.* 245: 499–512

Allen, D. A., Baines, D. W. T., Blades, J. C., Whittet, D. C. B. 1982. *MNRAS* 199: 1017–24

Allamandola, L. J., Tielens, A. G. G. M., Barker, J. R. 1989. *Ap. J. Suppl.* 71: 733–75

Arellano Ferro, A. 1984. *Publ. Astron. Soc. Pac.* 96: 641–45
Arquilla, R., Leahy, D. A., Kwok, S. 1986. *MNRAS* 220: 125–31
Bachiller, R., Gomez-Gonzalez, J., Bujarrabal, V., Martin-Pintado, J. 1988. *Astron. Astrophys.* 196: L5–8
Bachiller, R., Bujarrabal, V., Martin-Pintado, J., Gomez-Gonzalez, J. 1989. *Astron. Astrophys.* 218: 252–56
Bachiller, R., Huggins, P. J., Cox, P., Forveille, T. 1992. *Astron. Astrophys.* In press
Barker, J. R., Allamandola, L. J., Tielens, A. G. G. M. 1987. *Ap. J.* 315: L61–65
Barlow, M. 1993. In *Astronomical Infrared Spectroscopy: Future Observational Directions*, ed. S. Kwok. San Francisco: ASP Conf. Ser. 40: 97–109
Bedijn, P. J. 1987. *Astron. Astrophys.* 186: 136–52
Bidelman, W. P. 1985. *Bull. Am. Astron. Soc.* 17: 841–42
Bidelman, W. P. 1986. In *IAU Symp. 122: Circumstellar Matter*, ed. I. Appenzeller, C. Jordan, pp. 217–18. Dordrecht: Reidel
Blöcker, T. 1989. Diplom thesis. Univ. Kiel
Bond, H. E., Carney, B. W., Grauer, A. D. 1984. *Publ. Astron. Soc. Pac.* 96: 176–78
Bond, H. E., Luck, R. E. 1987. In *IAU Colloq. 95: The Second Conference on Faint Blue Stars*, ed. A. G. D. Philips, D. S. Hayes, J. W. Liebert, pp. 527–30. Schenectady: L. Davis
Bowers, P. F. 1990. In *Cool Stars, Stellar Systems, and the Sun*, ed. G. Wallerstein, ASP Conf. Series 9: 417–28
Bowers, P. F., Knapp, G. R. 1992. *Ap. J.* In press
Bujarrabal, V., Bachiller, R., Alcolea, J., Martin-Pintado, J. 1988. *Astron. Astrophys.* 206: L17–19
Bujarrabal, V., Alcolea, J., Planesas, P. 1992. *Astron. Astrophys.* 257: 701–14
Buss, R. H., Cohen, M., Tielens, A. G. G. M., Werner, M. W., Bregman, J. D., et al. 1990. *Ap. J.* 365: L23–26
Carsenty, U., Solf, J. 1982. *Astron. Astrophys.* 106: 307–10
Chan, J., Kwok, S. 1990. *Astron. Astrophys.* 237: 354–68
Cernoicharo, J., Guélin, M., Martin-Pintado, J., Penalver, J., Mauersberger, R. 1989. *Astron. Astrophys.* 222: L1–4
Cohen, M., Barlow, M. J. 1974. *Ap. J.* 193: 401–18
Cohen, M., Anderson, C. M., Cowley, A., Coyne, G. V., Fawley, W., et al. 1975. *Ap. J.* 196: 179–89
Cohen, M., Tielens, A. G. G. M., Allamandola, L. J. 1985. *Ap. J.* 299: L93–97
Cohen, M., Tielens, A. G. G. M., Bregman, J., Witteborn, F. C., Rank, D. M., et al. 1989. *Ap. J.* 341: 246–69
Cox, P. 1990. *Astron. Astrophys.* 236: L29–32
Crabtree, D., Rogers, C. 1993. In preparation
Crampton, D., Cowley, A. P., Humphreys, R. M. 1975. *Ap. J.* 198: L135–37
Davis, L. E., Seaquist, E. R., Purton, C. R. 1979. *Ap. J.* 230: 434–41
de Muizon, M., Geballe, T. R., d'Hendecourt, L. B., Baas, F. 1986. *Ap. J.* 306: L105–8
Dougados, C., Rouan, D., Lacombe, F., Forveille, T., Tiphense, D. 1990. *Astron. Astrophys.* 227: 437–46
Dougados, C., Rouan, D., Léna, P. 1992. *Astron. Astrophys.* 253: 464–74
Duley, W. W., Williams, D. A. 1981. *MNRAS* 196: 269–74
Ferni, J. D. 1981. *Ap. J.* 243: 576–82
Forveille, T., Morris, M., Omont, A., Likkel, L. 1987. *Astron. Astrophys.* 176: L13–16
Gammie, C. F., Knapp, G. R., Young, K., Phillips, T. G., Falgarone, E. 1989. *Ap. J.* 345: L87–89
Gatley, I. 1988. *Science* 242: 1217–1348
Geballe, T. R., Kim, Y. H., Knacke, R. F., Noll, K. S. 1988. *Ap. J.* 326: L65–68
Geballe, T. R., van der Veen, W. E. C. J. 1990. *Astron. Astrophys.* 235: L9–12
Geballe, T. R., Tielens, A. G. G. M., Kwok, S., Hrivnak, B. J. 1992. *Ap. J.* 387: 89–91
Gehrz, R. D. 1972. *Ap. J.* 178: 715–25
Gehrz, R. D., Woolf, N. J. 1970. *Ap. J.* 161: L213–17
Gillett, F. C., Low, F. J., Stein, W. A. 1967. *Ap. J.* 183: 87–93
Gillett, F. C., Hyland, A. R., Stein, W. A. 1970. *Ap. J.* 162: L21–24
Gillett, F. C., Backman, D. E., Beichman, C., Neugebauer, G. 1986. *Ap. J.* 310: 842–52
Heiligman, G. M. 1986. *Ap. J.* 308: 306–13
Herman, J., Baud, B., Habing, H. J. 1985. *Astron. Astrophys.* 144: 514–15
Hrivnak, B. J., Kwok, S. 1991a. *Ap. J.* 368: 564–69
Hrivnak, B. J., Kwok, S. 1991b. *Ap. J.* 371: 631–35
Hrivnak, B. J., Kwok, S., Volk, K. 1988. *Ap. J.* 331: 832–37
Hrivnak, B. J., Kwok, S., Volk, K. 1989. *Ap. J.* 346: 265–76
Hrivnak, B. J., Kwok, S., Geballe, T. R. 1993. *Ap. J.* Submitted
Hrivnak, B. J., Woodsworth, A. W. 1993. In *IAU Symp. 151: Planetary Nebulae*, ed. R. Weinberger, A. Acker. Dordrecht: Kluwer. In press
Hu, J. Y., Slijkhuis, S., de Jong, T., Jiang, B. W. 1992a. *Astron. Astrophys.* Submitted
Hu, J. Y., Slijkhuis, S., Nguyen-Q-Rieu, de Jong, T. 1992b. *Astron. Astrophys.* Submitted

Hu, J. Y., te Lintel Hekkert, P., Slijkhuis, S., Baas, F., Sahai, R. 1992c. *Astron. Astrophys.* Submitted
Huggins, P. J., Healy, A. P. 1989. *Ap. J.* 346: 201–11
Iyengar, K. V. K. 1986. *Astron. Astrophys.* 158: 89–96
Jaminet, P. A., Danchi, W. C., Sandell, G., Sutton, E. C. 1992. *Ap. J.* 400: 535–50
Jourdain de Muizon, M., d'Hendecourt, L. B., Geballe, T. R. 1990. *Astron. Astrophys.* 235: 367–78
Jura, M. 1986. *Ap. J.* 309: 732–36
Knapp, G. R. 1986. *Ap. J.* 311: 731–41
Knapp, G. R., Morris, M. 1985. *Ap. J.* 292: 640–69
Knapp, G. R., Phillips, T. G., Leighton, R. B., Lo, K. Y., Wannier, P. G., et al. 1982. *Ap. J.* 252: 616–34
Knapp, G. R., Sandell, G., Robson, E. I. 1993. Preprint
Kwok, S. 1980. *Ap. J.* 236: 592–97
Kwok, S. 1982. *Ap. J.* 258: 280–88
Kwok, S. 1987. In *Late Stages of Stellar Evolution*, ed. S. Kwok, S. R. Pottasch, pp. 321–35. Reidel: Dordrecht
Kwok, S. 1990. *MNRAS* 244: 179–83
Kwok, S., Feldman, P. A. 1981. *Ap. J.* 247: L67–71
Kwok, S., Bignell, R. C. 1984. *Ap. J.* 276: 544–50
Kwok, S., Purton, C. R., FitzGerald, P. M. 1978. *Ap. J.* 219: L125–27
Kwok, S., Hrivnak, B. J., Milone, E. F. 1986. *Ap. J.* 303: 451–64
Kwok, S., Hrivnak, B. J., Boreiko, R. T. 1987. *Ap. J.* 312: 303–13
Kwok, S., Volk, K., Hrivnak, B. J. 1989. *Ap. J.* 345: L51–54
Kwok, S., Hrivnak, B. J., Volk, K. M. 1990. In *From Miras to Planetary Nebulae*, ed. M. O. Mennessier, A. Omont, pp. 435–48. Gif-sur-Yvette: Ed. Frontiers
Kwok, S., Hrivnak, B. J., Geballe, T. R. 1993. In preparation
Lamers, H. J. G. L. M., Waters, L. B. F. M., Garmany, C. D., Perez, M. R., Waelkens, C. 1986. *Astron. Astrophys.* 154: L20–22
Langill, P. P., Kwok, S., Hrivnak, B. J. 1993. In *IAU Symp. 151: Planetary Nebulae*, ed. R. Weinberger, A. Acker. Dordrecht: Kluwer. In press
Latter, W. B., Maloney, P. R., Kelly, D. M., Black, J. H., Rieke, G. H., Rieke, M. J. 1992. *Ap. J.* 389: 347–56
Léger, A., Puget, J. L. 1984. *Astron. Astrophys.* 137: L5–8
Lequeux, J., Jourdain de Muizon, M. 1990. *Astron. Astrophys.* 240: L19–22
Lewis, B. M. 1989. *Ap. J.* 338: 234–43
Lewis, B. M., Eder, J., Terzian, Y. 1985. *Nature* 313: 200–2
Lewis, B. M., Eder, J., Terzian, Y. 1990. *Ap. J.* 362: 634–51
Likkel, L. 1989. *Ap. J.* 344: 350–70
Likkel, L., Omont, A., Morris, M., Forveille, T. 1987. *Astron. Astrophys.* 173: L11–14
Likkel, L., Forveille, T., Omont, A., Morris, M. 1988. *Astron. Astrophys.* 198: L1
Likkel, L., Forveille, T., Omont, A., Morris, M. 1991. *Astron. Astrophys.* 246: 153–74
Lo, K. Y., Bechis, K. P. 1976. *Ap. J.* 205: L21–25
Loup, C., Forveille, T., Nyman, L. Å., Omont, A. 1990. *Astron. Astrophys.* 227: L29–32
Marten, H., Szczerba, R., Blöcker, T. 1993. In *IAU Symp. 151: Planetary Nebulae*, ed. R. Weinberger, A. Acker. Dordrecht: Kluwer. In press
Mathis, J. S., Lamers, H. J. G. L. M. 1992. *Astron. Astrophys.* 259: L39–42
Meixner, M., Skinner, C. J., Temi, P., Rank, D., Bregman, J., et al. 1993. *Ap. J.* In press
Menzies, J. W., Whitelock, P. A. 1988. *MNRAS* 233: 697–703
Moseley, H. 1980. *Ap. J.* 238: 892–904
Mufson, S. L., Lyon, J., Marionni, P. A. 1975. *Ap. J.* 201: L85–89
Ney, E. P., Merrill, K. M., Becklin, E. E., Neugebauer, G., Wynn-Williams, C. G. 1975. *Ap. J.* 198: L129–34
Nyman, L.-Å., Booth, R. S., Curlström, U., Habing, H. J., Heske, A., et al. 1992. *Astron. Astrophys. Suppl.* 93: 121–50
Odenwald, S. F. 1986. *Ap. J.* 307: 711–22
Olofsson, H. 1987. In *Late Stages of Stellar Evolution*, ed. S. Kwok, S. R. Pottasch, pp. 149–63. Dordrecht: Reidel
Olofsson, H., Eriksson, K., Gustafsson, B. 1988. *Astron. Astrophys.* 196: L1–4
Omont, A., Moseley, S. H., Forveille, T., Glaccum, W., Harvey, P. M., Likkel, L. 1989. In *Proc. 22nd Eslab Symp. on Infrared Spectroscopy in Astronomy*, pp. 379–80. ESA SP-290
Omont, A., Loup, C., Forveille, T., te Lintel-Hekkert, P., Habing, H., Sivagnanam, P. 1992. *Astron. Astrophys.* In press
Omont, A., Moseley, S. H., Glaccum, W., Kwok, S., Harvey, P. M. 1993. In preparation
Oudmaijer, R. D., van der Veen, W. E. C. J., Waters, L. B. F. M., Trams, N. R., Waelkens, Ch., Engelman, E. 1992. *Astron. Astrophys. Suppl.* In press
Parthasarathy, M., Pottasch, S. R. 1986. *Astron. Astrophys.* 154: L16–19
Percy, J. R., Sasselov, D. D., Alfred, A., Scott, G. 1991. *Ap. J.* 375: 691–95
Perek, L., Kohoutek, L. 1967. *Catalog of Galactic Planetary Nebulae*. Prague. Czech. Inst. Sci.
Pottasch, S. R., Parthasarathy, M. 1988. *Astron. Astrophys.* 192: 182–86

Pottasch, S. R., Baud, B., Beintema, D., Emerson, J., Habing, H. J., et al. 1984. *Astron. Astrophys.* 138: 10–18
Pottasch, S. R., Bignell, C., Zijlstra, A. 1987. *Astron. Astrophys.* 177: L49–52
Preite-Martinez, A. 1989. In *IAU Symp. 131: Planetary Nebulae*, ed. S. Torres-Peimbert, pp. 9–16. Dordrecht: Kluwer
Preston, G. W., Krzeminski, W., Smak, J., Williams, J. A. 1963. *Ap. J.* 137: 401–30
Renzini, A. 1982. In *IAU Symp. 103: Planetary Nebulae*, ed. D. R. Flower, pp. 267–80. Dordrecht: Reidel
Roche, P. F., Aitken, D. K., Smith, C. H. 1991. *MNRAS* 252: 282–87
Rodriguez, L. F., Gomez, Y., Garcia-Barreto, J. A. 1985. *Rev. Mex. Astron. Astrofiz.* 11: 139–42
Russell, R. W., Soifer, B. T., Willner, S. P. 1977. *Ap. J.* 217: L149–53
Russell, R. W., Soifer, B. T., Willner, S. P. 1978. *Ap. J.* 220: 568–72
Sasselov, D. D. 1984. *Astrophys. Space Sci.* 102: 161–78
Schmidt, G. D., Cohen, M. 1981. *Ap. J.* 246: 444–54
Schönberner, D. 1983. *Ap. J.* 272: 708–14
Slijkhuis, S. 1992. PhD thesis. Univ. Amsterdam
Smith, M. G., Geballe, T. R., Sandell, G., Aspin, C. 1990. In *Submillimetre Astronomy*, ed. G. D. Watt, A. S. Webster, pp. 29–30. Dordrecht: Kluwer
Sourisseau, C., Coddens, G., Papoular, R. 1992. *Astron. Astrophys.* 254: L1–4
Sowell, J. R. 1990. *Astron. J.* 100: 834–48
Sun, J., Kwok, S. 1987. *Astron. Astrophys.* 185: 258–66
te Lintel Hekkert, P. 1990. PhD thesis. Univ. Leiden, Netherlands
te Lintel Hekkert, P., Chapman, J. M., Zijlstra, A. A. 1992. *Ap. J.* 390: L23–26
Trams, N. R. 1991. PhD thesis. Rijksuniv. Utrecht, Netherlands
Trams, N. F., Waters, L. B. F. M., Waelkens, C., Lamers, H. J. G. L. M., van der Veen, W. E. C. J. 1989. *Astron. Astrophys.* 218: L1–4
Trams, N. R., van Hoof, P. A. M., van de Steene, G. C. M. 1992. *Astron. Astrophys.* In press
van der Veen, W. E. C. J. 1988. Thesis. Leiden Obs., Netherlands
van der Veen, W. E. C. J., Geballe, T. R., Habing, H. J., van Langevelde, H. J. 1989a. *Astron. Astrophys.* 216: L1–4
van der Veen, W. E. C. J., Habing, H. J., Geballe, T. R. 1989b. *Astron. Astrophys.* 226: 108–36
van der Veen, W. E. C. J., Waters, R., Trams, N., Matthews, H. E. 1992. *Astron. Astrophys.* Submitted
van der Veen, W. E. C. J., Waters, R., Trams, N. 1993. In *High Galactic Latitude Supergiants*, ed. D. D. Sasselov. San Francisco: ASP Conf. Ser. In press
Volk, K. 1992. *Ap. J. Suppl.* 80: 347–68
Volk, K., Cohen, M. 1990. *Astron. J.* 100: 485–510
Volk, K., Kwok, S. 1987. *Ap. J.* 315: 654–65
Volk, K., Kwok, S. 1988. *Ap. J.* 331: 435–62
Volk, K., Kwok, S. 1989. *Ap. J.* 342: 345–63
Volk, K., Leahy, D. A. 1992. In *IAU Symp. 151: Planetary Nebulae*, ed. R. Weinberger, A. Acker. Dordrecht: Kluwer. In press
Volk, K., Kwok, S., Stencel, R. E., Brugel, E. 1991. *Ap. J. Suppl.* 77: 607–45
Volk, K., Kwok, S., Langill, P. L. 1992. *Ap. J.* 391: 285–94
Waelkens, C., Waters, L. B. F. M., Cassatella, A., Le Bertre, T., Lamers, H. J. G. L. M. 1987. *Astron. Astrophys.* 181: L5–8
Waters, L. B. F. M., Trams, N. R., Waelkens, C. 1992. *Astron. Astrophys.* 262: L37
Waters, L. B. F. M., Waelkens, C., Trams, N. R. 1993. In *Mass Loss on the AGB and Beyond*, ed. H. E. Schwarz. Garching: ESO. In press
Westbrook, W. E., Becklin, E. E., Merrill, K. M., Neugebauer, G., Schmidt, M. Willner, S. P., Wynn-Williams, C. G. 1975. *Ap. J.* 202: 407–14
Woodsworth, A. W., Kwok, S., Chan, S. J. 1990. *Astron. Astrophys.* 228: 503–5
Young, K., Serabyn, E., Phillips, T. G., Knapp, G. R., Güsten, R., Schulz, A. 1992. *Ap. J.* 385: 265–72
Zhang, C. Y., Kwok, S. 1990. *Astron. Astrophys.* 237: 479–94
Zhang, C. Y., Kwok, S. 1991. *Astron. Astrophys.* 250: 179–211
Zhang, C. Y., Kwok, S. 1992. *Ap. J.* 385: 255–64
Zijlstra, A. A., Gaylard, M. J., te Lintel Hekkert, P., Menzies, J., Nyman, L.-Å., Schwarz, H. E. 1991. *Astron. Astrophys.* 243: L9–12
Zijlstra, A. A., Pottasch, S. R., Bignell, R. C. 1989a. *Astron. Astrophys. Suppl.* 79: 329–57
Zijlstra, A. A., te Lintel Hekkert, P., Pottasch, S. R., Caswell, J. L., Ratag, M., Habing, H. J. 1989b. *Astron. Astrophys.* 217: 157–78
Zuckerman, B., Dyck, H. M. 1986a. *Ap. J.* 304: 394–440
Zuckerman, B., Dyck, H. M. 1986b. *Ap. J.* 311: 345–59